Characterizing Genetic Mechanisms Involved in Measuring Day-length in *Drosophila melanogaster*

Harjit Khaira[1] and Kwangwon Lee[1,2*]

[1] Department of Biology, Rutgers, The State University of New Jersey, Camden, New Jersey, United States of America

[2] Center for Computational & Integrative Biology, Rutgers, The State University of New Jersey, Camden, New Jersey, United States of America

Short Title: *PKCdelta* on Photoperiodism

[*] Corresponding author

E-mail: kwangwon.lee@rutgers.edu

Abstract

Many organisms are known to regulate seasonal behaviors and physiological processes in response to day length changes through photoperiodism. Extreme changes in photoperiods have detrimental effects on human health, which can impair development and serve as the origin of adult diseases. Since the seminal work by Bünning in 1936, there are studies supporting the view that organisms can measure the day length through an endogenous 24-hour cellular circadian clock. However, the mechanisms involved in measuring seasonal or day-length changes are not understood. In the current study, we performed a genome-wide association study (GWAS) on photoperiodism using the *Drosophila* Genetic Reference Panel. The GWAS identified 32 candidate genes responsible for photoperiodic regulations. The knockout mutants of the top four candidate genes (*Protein Kinase C delta (Pkcdelta), Glucuronyltransferase-P* (*GlcAT-P*), *Brain-specific homeobox* (*Bsh*), and *Diuretic hormone 31 Receptor (Dh31-R1))* were analyzed for their photoperiod and circadian period phenotypes. *PKCdelta* and *GlcAT-P* mutants show a significantly different photoperiod response compared to that of the wild type strain, and also had an altered circadian period phenotype. Further molecular characterization revealed that the mutant two independent mutant alleles of *PKCdelta* with a defective catalytic domain had distinct photoperiod responses. Taken these data together, we concluded that there is overlap between the circadian clock and photoperiodic regulations in *Drosophila*, and *PKCdelta* is a component that is involved in both circadian and photoperiodic regulations. By identifying novel molecular components of photoperiod, the current study provides new insights into the genetic mechanisms of determining the seasonal changes.

Keywords Photoperiodism; Circadian Clock; GWAS; *Drosophila*

47

48 **Introduction**

49 Most organisms experience predictable environmental changes; daily, tidal, lunar, and seasonal.
50 These changes mean different availability of resources and stressors at predictable time intervals.
51 It is crucial for an organism to prepare for the incoming season for its survival in nature. Thus, it
52 is not surprising that organisms have evolved time-measuring cellular devices. Among the known
53 biological rhythms, seasonal rhythm plays a major role in many biological processes such as
54 growth, development, reproduction, migration, and dormancy. A robust response to these rhythms
55 can increase the survival success of an organism (Bradshaw and Holzapfel, 2010). However, little
56 is known about the molecular and genetic mechanism of how an organism interprets and adapts to
57 seasonal environmental changes.

58 Photoperiodism is the physiological response of an organism to changes in day length.
59 Photoperiod is one of the most important factors that control seasonal breeding. Few species show
60 extreme behaviors like hibernation while many species synchronize breeding and birth of their
61 offspring to the most advantageous time of the year for better survival. Based on the gestation
62 period, photoperiodic species can be categorized as long day (LD) or short day (SD) breeders.
63 Animals like sheep and goats with long gestation periods begin to breed as day length decreases,
64 while animals like mice and hamsters breed as day length increases (Ortavant et al., 1964). In
65 humans there are some psychological and psychiatric consequences in response to the
66 photoperiodic changes. There also is seasonality in birth rates among humans and onset of certain
67 diseases like measles in the population (Martinez-Bakker et al., 2014). Patients with bipolar
68 disorders have more depressive episodes during the late autumn and early winter, while there is an
69 increase of manic episodes during spring and summer (Maruani et al., 2018). In flowering plants,

70 some are flowering at specific season of the year, and thus grouped as SD or LD flowering plants.
71 The molecular and genetic pathways of photoperiodism have been studied in plants (Johansson
72 and Staiger, 2015). It is also known that the circadian clock controls the activity of CONSTANS
73 (CO), which is a key component of the photoperiod pathway. CO activates the transcription
74 of *FLOWERING LOCUS T* (*FT*) which the ultimately leads to flowering in plants (Song et al.,
75 2010).

76 Photoperiodic responses are well documented in insects (Bradshaw and Holzapfel, 2010).
77 Although *Drosophila melanogaster* is the successful model species for many biological processes,
78 the species was regarded as less optimal for studying photoperiodism due do a less pronounced
79 photoperiod response (Tauber and Kyriacou, 2001). Most of the studies of photoperiodism in
80 insects utilized the diapause as a phenotype. Diapause occurs when female insect ovaries shrink
81 due to photoperiod changes as an indicator of photoperiodic phenotype. On the contrary to the
82 concern in using *D. meanogaster* for studying photoperiodism, it also has been shown that *D.*
83 *melanogaster* has a robust photoperiod response under semi-natural or SD conditions (Nagy et al.,
84 2018; Saunders et al., 1989).

85 One compelling hypothesis regarding the seasonal rhythm is that an organism can
86 'interpret' the season by measuring the day length. A crucial assumption is that an organism knows
87 the season by measuring photoperiods is due to the presence of an endogenous cellular daily clock,
88 called the circadian clock. Circadian clocks are endogenous timekeeping networks that drive 24hr
89 circadian rhythms. Bünning reported that the rate of leaf movement speed changes during different
90 seasons and proposed the circadian clock controlled this via photoperiodism (Bünning, 1936).
91 Since then, a number of studies supported Bunning's hypothesis in certain organisms while
92 rejecting his hypothesis in others. Studies on aphids and spider mites conclude that their

93 photoperiod mechanisms do not seem to depend on endogenous 24-h rhythms (Lees, 1960).
94 Mutation of the classical clock gene *period* (*per)* still allowed *D. melanogaster* to distinguish
95 between SD and LD . It was concluded that the clock gene *per* cannot be involved in night-length
96 measurement mechanism (Saunders, 1990). However, another study in *Drosophila* suggests that
97 the circadian clock is necessary for a photoperiodic response, as arrhythmic clock mutants per^{01},
98 tim^{01}, and Clk^{JRK} have altered photoperiodic responses from wild-type *Drosophila* (Pegoraro et al.,
99 2014). For the last few decades, the genetic and molecular mechanisms of circadian clocks have
100 been characterized in many organisms (Partch et al.2014, Nohales and Kay 2016). However, it is
101 still not well understood on how the circadian clock is involved in measuring photoperiodism or
102 day length changes.

103 There are at least two different hypotheses on how circadian clocks are involved in
104 measuring seasonal changes: the external coincidence model and the internal coincidence model.
105 In the external coincidence model, the photoperiodic response can be generated by the circadian
106 clock that is sensitive to light at certain phases (Sawa et al., 2008). If the light signal is detected at
107 this sensitive phase, then the photoperiodic response will be displayed such as flowering in plants.
108 Light can entrain the clock and set the phase of photoperiodic response like flowering, but light
109 can also directly induce flowering. In the internal coincidence model, two (or more) rhythms are
110 produced by the clock. Under the internal coincidence model, responses, such as flowering, are
111 only generated in conditions that bring both rhythms in phase with each other (Sawa et al., 2008).
112 Various studies show one or the other hypotheses at work in a range of organisms. In *Arabidopsis*,
113 external coincidence models can explain long day-specific dusk *FT* (a florigen gene) expression
114 (Song et al., 2018). Studies using the parasitic wasp *Nasonia vitripennis* support the internal
115 coincidence model. Using the Nanda-Hamner protocol it was found that *N.vitripennis* exhibit two

116 peaks in diapause, a dawn and dusk peak, which is suggestive of two circadian oscillators
117 (Saunders, 2012). In some bacterial species the hourglass model is suggested to be responsible for
118 timekeeping (Johnson et al., 2017). When bacteria exposed to more regular environmental
119 conditions such as consistent light-dark cycles or constant photoperiod, hourglass model is at play.
120 However, when the environmental conditions vary such as inconsistent light-dark cycles or
121 photoperiods leads to a sustained oscillator (Johnson et al., 2017).

122 In our current study, we aim to better understand the genetic mechanisms of
123 photoperiodism and the roles of circadian clocks in photoperiodism using the eukaryotic model
124 organism *D. melanogaster*. *Drosophila* Genetic Reference Panel (DGRP) is a community resource
125 of 205 inbred lines created from 40 wild type parents for studying population genomics and
126 quantitative traits (Mackay et al., 2012). Because the DGRP is inbred to homozygosity, it is
127 possible to identify SNP variants responsible for the trait of interest. DGRP is a fully sequenced
128 population with annotated high-quality SNPs, indels, and chromosomal inversions (Huang et al.,
129 2014; Mackay et al., 2012). DGRP has been used to study various complex traits such as starvation
130 resistance, startle response, chill coma recovery (CCR) time, and circadian behavior (Mackay et
131 al., 2012; Harbison et al., 2019).

132 Although diapause has been the phenotype of choice in characterizing the photoperiodic
133 response, the diapause assay is challenging to perform in a high throughput manner. Therefore, we
134 optimized the CCR assay as a phenotype for an organism's ability to respond to the photoperiodic
135 changes to perform the initial DGRP Genome-Wide Association Study (GWAS). We propose that
136 our approach would identify genes involved in both photoperiodism and the circadian clock or
137 only in photoperiodism. Our current study identified 32 candidate photoperiod genes from which
138 we assessed the photoperiod response of the top 4 genes using CCR. We further characterized the

139 role of allelic mutants of *PKCdelta* in photoperiodism using CCR, diapause, and molecular
140 techniques.
141
142 **Materials and Methods**
143 *Fly stocks*
144 We purchased the DGRP strains from the Bloomington Drosophila Stock Center (Indiana
145 University, Bloomington, IN). In the laboratory, the fly stock was maintained at room temperature
146 (25°C) and in 12L:12D photoperiod conditions. The following are the *PKCdelta* mutants
147 BDSC#18258 Pbac[RB]PKCdelta[e04408], BDSC#59433 Mi[MIC]PKCdelta[MI13377]. The
148 BDSC#62582 is *GlcAT-P* knockout mutant Pbac[GlcAT-P]0027-G4, BDSC#27467 Bsh mutant
149 EPbsh[G3075]. BDSC#22718 is the *Dh31-R1* knockout mutant ET1Dh31-R1[MB00175].
150
151 *Photoperiod conditions and Chill coma recovery*
152 Chill Coma Recovery (CCR) is a traditional method used to assess the photoperiod phenotype in
153 *Drosophila* species. CCR is expressed as the time (in seconds) it takes an organism to recover from
154 a paralysis like state after being kept under extremely low temperature. *D. melanogaster* enter the
155 chill coma at 7.0 ± 0.9 °C (Hosler et al., 2000). It has been clearly demonstrated that flies raised
156 under short-day (SD) photoperiod conditions compared to long-day (LD) photoperiod conditions
157 have an advanced (or shorter) recovery time (Lanciani et al., 1992). DGRP fly lines were reared
158 under LD and SD in a chamber, 25 ± 0.5 °C and 70% humidity. The LD consisted of 16 hours of
159 light and 8 hours of dark (16h:8h), while the SD consisted of 8 hours of light and 16 hours of dark
160 (8h:16h). The flies were reared under these conditions for two weeks. Chill coma was then
161 performed by placing the flies in 4 °C for 60 minutes. Next, the flies were placed into 5 mm glass

162 tubes and into the *Drosophila* activity monitors (DAM2, Trikinetics) to measure the time it takes
163 for the flies to recover. For an accurate measure of the recovery time, the flies were placed in the
164 middle of the glass tube near the IR sensor to capture the exact time the fly recovered from the
165 coma.
166
167 *Diapause Assay*
168 The diapause assay was performed by surgically removing the ovaries after rearing female flies
169 under different photoperiods. Previous research suggested that female *Drosophila* placed under
170 SD enter reproductive diapause which results in underdeveloped ovaries. The SD chamber
171 condition mimics the winter-like days when most organisms cease to reproduce to conserve
172 energy, therefore, diapause is induced in female flies (Saunders et al., 1989). Female *Drosophila*
173 placed under LD condition do not enter diapause. The *PKCdelta* mutants, *PKCdelta*:Pbac and
174 *PKCdelta*:MIC were reared under SD and LD photoperiodic conditions along with DGRP208
175 (WT) strain as a control. Newly hatched female flies were placed under the photoperiod conditions
176 for 12 days, 25˚ C. Overies were dissected in 1x PBS, the image was taken with a light microscope
177 (LEICA microsystems, LEICA EC3, Model:MEB126) under 4x magnification.
178
179 *qPCR*
180 The expression level of the candidate gene *PKCdelta* was characterized under SD and LD. The
181 RNA was prepared using the Zymo Research Direct-Zol RNA extraction kit (Cat#R2050). The
182 cDNA was prepared using the New England Biolabs (NEB) protoscript II first strand cDNA
183 synthesis kit (Cat#E65605). For qPCR the Applied Biosytems PowerUp SYBER Green master
184 mix was used (Cat#A25742) in the Applied Biosystems QuantStudio 6 Rlex Real-Time PCR

185 system according to the manufacture's manual. The following primer set was used; ACTIN served
186 as a control, (Fw; GCAAGTACTCTGTCTGGATC) (Rv; CCAGCAGAATCAAGACCATCC).
187 HK-5 primer set which targeted the RD transcript of *PKCdelta* (Fw;
188 CGATCGATTGGGGTTTGCTGG) (Rv:GTGATGTGAGGATTTGTGTAGG), expected
189 product size 283 bp. HK6 primer set targeted the RE transcript of *PKCdelta* (Fw;
190 TCGAGCTGAAGACAACACCT) (Rv: CTTTCTTAGCTTCGACTTGGTT) expected to product
191 size 160bp (Figure S4, Table S2).

192

193 *Statistical Analysis*

194 *Cohen's D*

195 CCR has been used successfully by other groups as the phenotype reflecting photoperiodic
196 response (Pegoraro et al., 2014). Our primary interest is measuring the 'differential' response of
197 each genotype to two different photoperiodic conditions. Cohen's D (CD) is used to measure the
198 effect size of the photoperiodic response in each genotype (Lakens, 2013):

199 $$CD = \frac{(CCR_{SD} - CCR_{LD})}{Average(STDV_{CCR_{SD}}, STDEV_{CCR_{LD}})}$$

200 For each of the DGRP strains, the average CCR time was calculated from 20 replicates per
201 strain in SD (CCR_{SD}) and LD (CCR_{LD}). The CD value of each genotype was calculated by
202 subtracting CCR_{LD} from CCR_{SD}, and divided by the average of the two standard deviations of
203 CCR_{LD} and CCR_{SD}. The CD values can be divided into three groups: large effect size, CD > 0.8;
204 medium effect size, 0.8 > CD > 0.5; and small effect size, CD < 0.2. The CD values for the mutants
205 were obtained by subtracting equinox photoperiod CCR value from that of SD or that of LD
206 respectively. This was done to ensure that the data was normalized to the EQ photoperiod.

207

208 $$CD_{SD} = \frac{(CCR_{SD} - CCR_{EQ})}{Average(STDV_{CCR_{SD}\&EQ})} \quad , CD_{LD} = \frac{(CCR_{LD} - CCR_{EQ})}{Average\left(STDEV_{CCR_{LD\&EQ}}\right)}$$

209 CD value provides directionality by positive or negative values. Thus, CD value shows if a
210 photoperiodic condition provided a positive effect on the strain or a negative effect in the CCR
211 assay.

212

213 *Genotype Effect Size*

214 To measure the difference between the effect size of CD in different genotypes, we calculated the
215 Genotype Effect Size (GES) by subtracting the CD value of the wild type from that of the mutant.

216 $$CD_{GenotypeX} - CD_{Wild\ type} = Genetic\ Effect\ Size\ (GES)$$

217 In calculating the GES values, DGRP208 (WT) was used as the baseline. GES value allowed us
218 to determine which candidate gene had the most differential response to the photoperiod in
219 comparison to that of the wild type.

220

221 *GWAS Analysis*

222 After calculating CD for all the strains under different photoperiodic conditions, we performed the
223 GWAS using the web-based tool provided by DGRP2 (Mackay et al., 2012; Huang et al., 2014).
224 The 1,881,979 select SNPs were analyzed for their association with the photoperiod response. All
225 the variants from the GWAS were graphed in a manhattan plot with their chromosome on the X-
226 axis and -log10(p) of the p values on the Y-axis. There are two significant thresholds -log10(5e-5)
227 and -log10(5e-8) (Figure 2). The SNPs above the -log10(5e-8) were considered significant SNPs.

228

229 *Heritability*

230 The HiLMM R package was used to calculate narrow-sense heritability of photoperiod response
231 in the DGRP population. The HiLMM package provides an estimation of heritability with
232 confidence intervals in linear mixed models.

233

234 **Results**

235 *Variation in CCR in the DGRP*

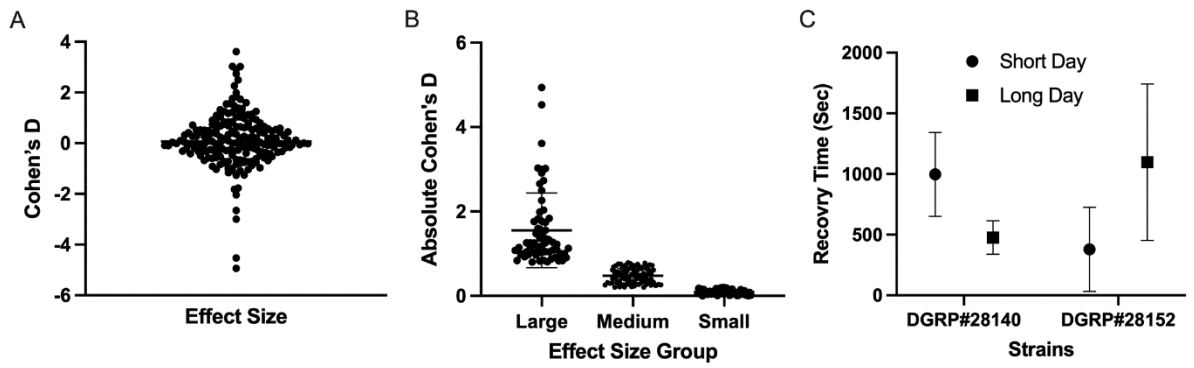

Figure 1. Variation in chill coma recovery in the DGRP population. A. The overall distribution of the CD values within the DGRP population, Shapiro-Wilks normality test p = 3.763e-09, $p < 0.05$, and W = 0.9194. B. The Cohen's D (CD) of the DGRP population, CD = (CCR_{SD} - CCR_{LD})/average (STDV_CCR_{SD}, STDV_CCR_{LD}). CD > 0.8 is large effect size, CD of 0.5 is medium effect size, and CD < 0.2 is small effect size. The majority of the DGRP strains fall under medium effect size total of 93 strains, while 63 strains fall under large effect size and 49 under small effect size. Thick horizontal lines represent mean and thin lines represent standard deviation. C. The CCR of the two representative strains from the DGRP population, DGRP28140 and DGRP28152 under Short Day (SD, circle) and Long Day (LD, square) photoperiods.

236
237 To test our hypothesis that genetic variations exist in photoperiodic response in *D. melanogaster*,
238 we analyzed the CCR phenotype in DGRP, and found significant variations in CCR among DGRP

239 strains (Figure 1, S1). The distribution of Cohen's D values in DGRP, Shapiro-Wilks p = 3.763e-
240 09, and W = 0.9194 (Figure 1A). To determine the differential response of each DGRP genotype
241 to the two different photoperiods, CD values were calculated for each genotype (Materials and
242 Methods). The majority of the DGRP strains fall under medium effect size (n = 93), large effect
243 size (n = 63), and small effect size (n= 49) (Figure 1B). There is more variation in CD values
244 among the large effect size DGRP strains than the strains that fall under medium and small effect
245 size. The overall average CCR in LD is 941 sec while CCR in SD is 1095 sec in the whole DGRP
246 population. Two representative strains are shown along with their recovery time under SD and LD
247 (Figure 1C). DGRP28140 has a delayed recovery time under SD in comparison to that of LD,
248 while DGRP28152 has a faster recovery time in SD compared to LD. To determine how much of
249 the variation is due to genetic factors in the DGRP population, we calculated the heritability.
250 Heritability (h^2) for the long day condition was 0.51 and h^2 for the short-day condition was 0.45.
251 It was previously reported that there is a sex difference in the CCR of *Drosophila* (Pegoraro et al.,
252 2014). However, there was no strong correlation between sex and CCR in our experimental
253 condition. The data from both sexes were grouped together for our GWAS analysis (Figure S2).
254
255 *GWAS Analysis for Photoperiodism*

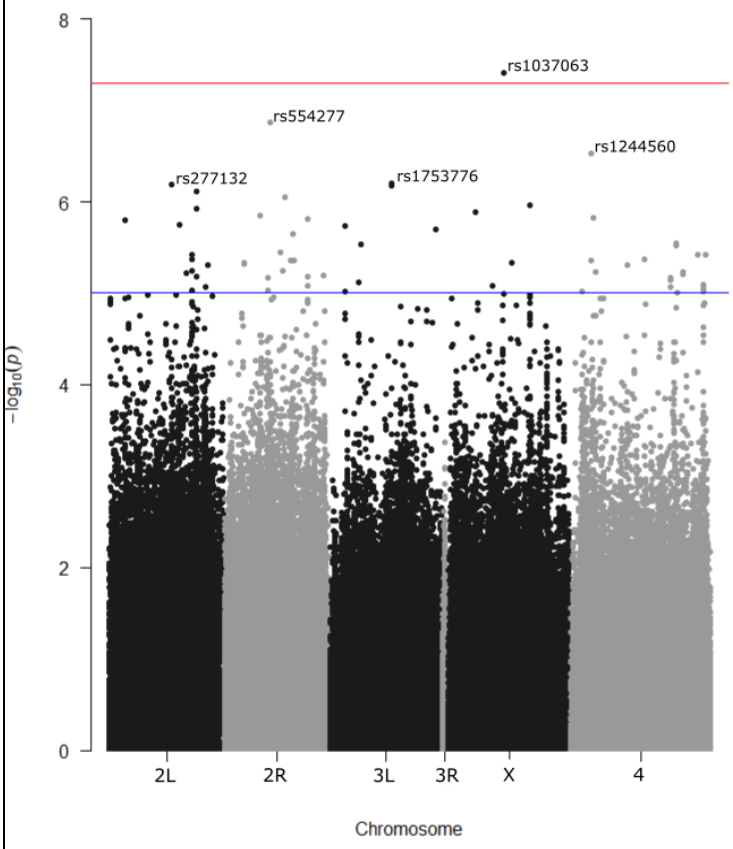

Figure 2. Manhattan plot for SNPs in the GWAS analysis. Each point represents a single SNP, and the height of the SNP represent the strength of association with photoperiod (CCR) response expressed as –log10(p). The horizontal lines represent the genome-wide Bonferroni significance threshold (blue line p = -log10(5e-5), red line p = -log10(5e-8). The variant rs1037063 is associated with GlcAT-P, rs554277 is associated with Dh31-R1, rs1753776 is associated with PKCdelta, rs277132 and rs1244560 are not associated with any particular gene since they are in the intergenic regions.

We performed GWAS analysis on CCR using it as a readout for photoperiodic response (Materials and methods) and identified genetic variants that were significant, p = 1E-07 (Figure 2). We also identified the 32 most promising variants strongly associated with the photoperiod response (Table S1). The enrichment analysis of these candidate genes shows a list of biological phenotypes including jumping, flight phenotypes, and circadian rhythms (Figure S3).

262 We characterized the top four candidate genes that are strongly associated with photoperiod
263 CCR responses, p ≥1E-07; *Glucuronyltransferase-P* (*GlcAT-P*); p = 6.63E-08, *Brain-specific*
264 *homeobox* (*Bsh*); p = 8.46E-07, *Protein Kinase C delta (Pkcdelta)*; p = 8.22E-07, and *Diuretic*
265 *hormone 31 Receptor (Dh31-R1)*; p = 3.49E-07. *GlcAT-P* belongs to the glycosyltransferase
266 family which are involved in catalyzing the conjugation of glucuronic acid from UDP-glucuronate
267 to an acceptor. This particular gene is involved in the biosynthesis of L2/HNK-1 carbohydrate
268 epitopes on both glycolipids and glycoproteins (Kim et al., 2003). *Bsh* encodes a putative
269 transcription factor, and it is needed for the specification of neural identities in the adult brain. The
270 rat ortholog of *Bsh* (*Bsx)* is suggested to be under circadian regulations and is expressed in the
271 mature pineal gland of rat (Carstensen et al., 2019). *Dh31-R1* is *Diuretic hormone 31 Receptor*
272 which encodes a protein that exhibits diuretic hormone receptor activity, and it is involved in G
273 protein-coupled receptor signaling pathways. *Dh31-R1* is also known to be involved in time
274 measurement and activity rhythms through the circadian clock system (Dubowy and Cavanaugh,
275 2014). *PKCdelta* belongs to a family PKC consisting of serine/threonine kinases which are
276 activated by extracellular signaling. PKCs are divided into subgroups of Classical PKCs, Novel
277 PKCs, and Atypical PKCs. *PKCdelta* belongs to the class of Novel PKCs which happen to be
278 known for their two C1 domain and activation via 1,2-diacylglycerol (DAG) and phosphatidyl-
279 serine (PS). While the cPKC family requires DAG and PS and aPKC only requires PS as a cofactor
280 for activation (Shieh et al., 2002; Suh et al., 2003). We identified two independent SNP variants
281 in *PKCdelta*, which strongly suggest that the alleles of *PKCdelta* is associated with the variation
282 of CCR in the DGRP population.
283
284 *Photoperiodic responses of the knockouts of the candidate genes*

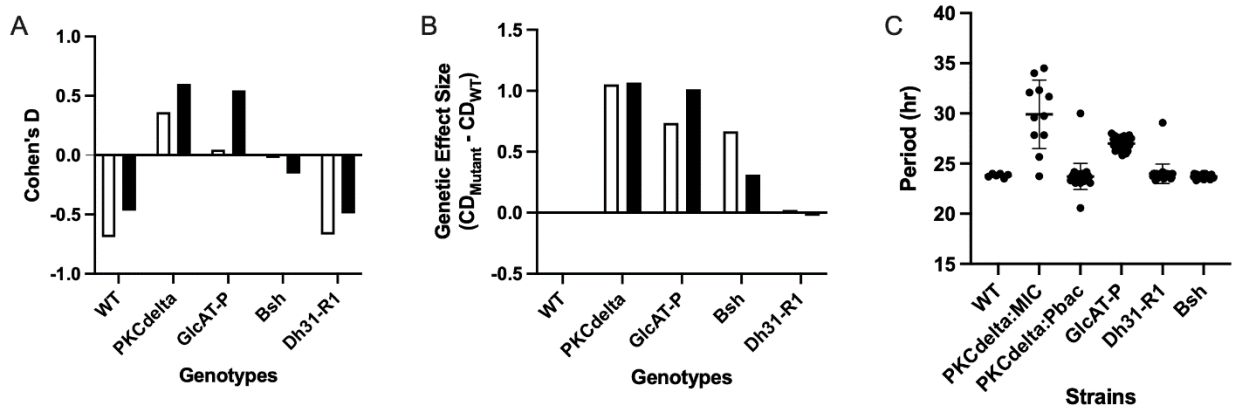

Figure 3. The photoperiod response and clock period phenotype of the top four candidate knockout strains A. Cohen's D values of the knockout mutants of the four candidate genes under LD and SD photoperiods compared to the wild type DGRP 208 strain (WT). The CD is normalized to equinox (EQ) photoperiod (Materials and Methods). The WT, *Dh31-R1* and *Bsh* have negative CD in LD (open) and SD (filled), while *PKCdelta* mutant *PKCdelta:*Pbac and *GlcAT-P* have positive CD under both conditions. B. The Genetic Effect Size of the candidate gene mutants, *PKCdelta:*Pbac and *GlcAT-P* mutants show a different photoperiod response compared to the WT under LD (open) and SD (filled). C. The circadian period of the candidate gene mutants compare to the WT with the period of 24 hr. *GlcAT-P* has a significantly longer period compared to WT (t-test: $p < 0.05$, $p = 1.16E-13$) and *PKCdelta:*MIC mutant of the *PKCdelta* has longer period compared to the WT (t-test: $p < 0.05$, $p = 1.28E-3$). Error bars represents standard deviation. N > 20.

To further characterize the top 4 candidate genes, first, we analyzed CCR response of the knockout strains; *PKCdelta* mutant PKCδ^{e04408} (BDSC# 18258), *GlcAT-P* mutant $GLCAT-P^{0027-G4}$ (BDSC#62582), *Bsh* mutant Bsh^{G3075} (BDSC#27467) and *Dh31-R1* mutant $Dh31-R^{MB00175}$ (BDSC#22718). As a control, one DGRP parent strain DGRP208 (WT) was used to compare

290 between the Cohen's D values. For this analysis equinox (EQ) condition, a 12:12 hr light:dark
291 cycle was used along with SD and LD photoperiods. The CD was obtained by subtracting (or
292 normalizing) the EQ photoperiod CCR from SD & LD CCR. The WT strain has a negative CD
293 value of -0.69 (Figure 3A). The *Dh31-R1* mutant has a similar photoperiod response to the WT
294 with negative CD values in both SD and LD photoperiod. *Bsh* mutant also has negative CD value
295 though the effect is not as exaggerated. Both *GlcAT-P* and *PKCdelta;Pbac* mutants has positive
296 CD values (Figure 3A). To determine how different these mutants' photoperiod responses were
297 from the WT control, the CD value of the WT was subtracted from the CD values of the mutant,
298 the final value is termed Genetic Effect Size (GES) (Figure 3B, Materials and Methods). *Bsh*,
299 *GlcAT-P* and *PKCdelta*:Pbac have different photoperiod responses compared to the WT with
300 *PKCdelta* being the most different. The GES of *PKCdelta*:Pbac is not significantly different
301 between LD and SD. However, *GlcAT-P, Bsh,* and *Dh31-R1* have a difference in GES between
302 LD and SD (Figure 3B).

303 Next, we tested the hypothesis that there are shared genetic regulators between the
304 circadian clock and photoperiodism. We examined the period of the candidate photoperiod knock
305 out genes using WT as a control (Figure 3C). Compared to the WT which had a period of 24 hr,
306 *GlcAT-P* and *PKCdelta*:MIC mutants have a significantly longer period (t-test: $p < 0.001$, $p<0.01$).
307 We concluded that *GlcAT-P* and *PKCdelta*:MIC genes play a role in both circadian clock
308 regulation and photoperiodism. We decided to investigate *PKCdelta* further for three reasons. The
309 two *PKCdelta* mutant alleles showed a significantly different photoperiodic CCR response from
310 that of the WT (Figure 3B), one of the allelic mutants of *PKCdelta* had an altered circadian period
311 (Figure 3C), and GWAS analysis showed that there are two independent SNP variants associated
312 with the photoperiodic CCR response for this gene (Figure 2 and File S3).

313

314 *PKCdelta Candidate Gene*

315 *PKCdelta* is a kinase known to be involved in cellular signaling pathways like cell growth,
316 apoptosis, tumor promotion and carcinogenesis (Suh et al., 2003). We examined two parental
317 DGRP strains one with a large positive CD value (DGRP379) and another with a large negative
318 CD value (DGRP391). *PKCdelta* transcribes three transcripts, RC, RD, and RE (Figure S4). The
319 transcripts RC and RD are similar to each other except with a slight difference in the UTR region;
320 the RD isoform has a shorter UTR region than the RC isoform. The RC and RD transcript have
321 regulatory domain which contain C2, C1 and pseudosubstrate domains toward the N-terminal.
322 Toward the C-terminal there is a catalytic kinase domain which is shared with all three isoforms
323 (Figure S5). There are two different transcription start sites, one that starts the beginning of
324 isoforms RD and RC, and the other starts at the RE isoform. The RE isoform is a nested gene with
325 its transcription start site residing in one of the introns of RC and RD transcripts (Kumar, 2009).

326 We found that there are two non-synonymous SNPs in the exon 6 which resides in the RE
327 transcript in the DGRP379 strain but not in DGRP391. The first SNP position is at 12445745:
328 Guanine to Adenosine, which changes Alanine to Threonine. The second SNP position is at
329 12446453: Guanine to Cytosine, which changes Alanine to Proline. The first SNP position is in a
330 ployQ region, which is conserved in the *Drosophila* species. The second SNP causes a repeat of
331 the sequence surrounding the region (Figure S6A, S6B). We found that RE isoform is a nested
332 gene which is only conserved in the *Drosophila* genus (Figure S7).

333

334 *Diapause and CCR in PKCdelta mutant alleles*

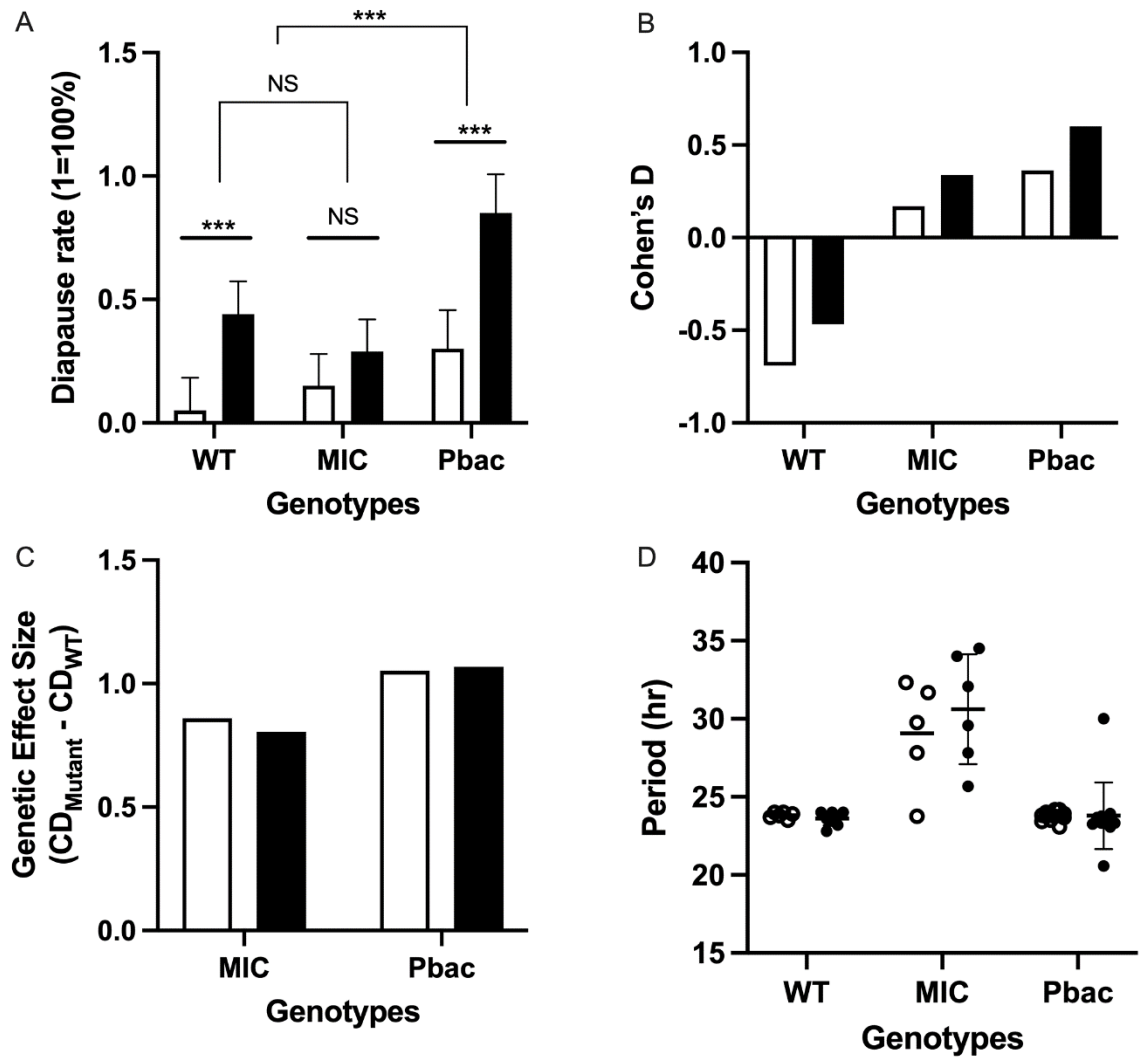

Figure 4. The photoperiod and period response of *PKCdelta:*MIC and *PKCdelta*:Pbac mutants compared to WT. A. The diapause response of candidate gene *PKCdelta* mutants compared to WT in LD (open) vs SD (filled). There is a significant difference in *PKCdelta*:Pbac mutant diapause response, compared to WT in both photoperiods (Z-test: p= 0.0014 (LD), 0.010 (SD)). *PKCdelta*:MIC diapause response compared to WT in each photoperiod is not significantly different (Z-test: p = 0.27 (LD), 0.30 (SD)). However, there is a significant difference in *PKCdelta*:Pbac LD and SD diapause response (Z-test p = 0.002) and in WT (Z-test: p = 0.007),

but not in *PKCdelta*:MIC (Z-test: $p = 0.29$). B. Cohen's D of *PKCdelta*;Pbac and *PKCdelta*;MIC compared to WT, the CD values were obtained by subtracting EQ CCR response from LD (open) and SD (filled) photoperiod response. WT has a negative CD, while *PKCdelta*:MIC and *PKCdelta*:Pbac are positive. C. GES of the mutants compared to the WT, both mutant alleles show significantly different photoperiod response from that of the WT, LD (open), SD (filled). D. Circadian period of the *PKCdelta* mutants compared to that of WT separated by homozygous females (open) and hemizygous males (filled). Error bars represent SD, $10 < n < 20$, homozygous vs hemizygous (t-test, $p > 0.05$).

To further explore the role of *PKCdelta* in photoperiodism, we performed the diapause assay using the *PKCdelta*:Pbac and *PKCdelta*:MIC allelic mutants under different photoperiodic conditions. The *PKCdelta*:Pbac mutant has an insertion of a *piggy bac* element in an intron close to the 3' end of the gene. The *PKCdelta:*MIC mutant has an insertion in the 5' end of the gene and contains a minos-based construct which was created by the Gene Disruption Project (GDP) (Venken et al., 2011) (Table S4). We found that both mutant alleles have a mutation in the catalytic domain of the enzyme *PKCdelta* (Figure S9, Table S3 and S4)

Using WT as a control, the diapause assay was carried out under SD and LD conditions (Figure 4A). As expected, the WT has increased diapause incidences under SD conditions compared to the LD condition (Z-test, $p < 0.05$). There was a significant difference in *PKCdelta*:Pbac mutant's diapause response compared to that of WT in both photoperiods (Z-test, $p = 0.0014$ (LD), $p = 0.01$ (SD)). The *PKCdelta*:MIC mutant's diapause response compared to WT in each photoperiod is not significantly different (Z-test, $p = 0.27$ (LD), $p = 0.30$ (SD)). However, there is a significant difference in *PKCdelta*:Pbac LD and SD diapause response (Z-test, p =

350 0.002), and in WT (Z-test, p = 0.007), but not in *PKCdelta*:MIC (Z-test, p = 0.29) (Figure 4A).
351 The diapause response in *PKCdelta*:MIC mutant is not statistically significant from that of the
352 WT. We interpreted this as the mutant allele *PKCdelta*:MIC cannot distinguish SD from LD
353 because the diapause response between photoperiods is not significantly different (Z-test: p =
354 0.29).

355 To determine the necessity of *PKCdelta* for the photoperiodic CCR response, we
356 preformed the CCR assay using the allelic mutants of *PKCdelta* (Figure 4B). The CD values of
357 *PKCdelta*:Pbac and *PKCdelta*:MIC are positive compared to WT. However, *PKCdelta*:MIC have
358 lower CD values from that of *PKCdelta*:Pbac. The GES of the mutants compared to the WT show
359 that *PKCdelta*:Pbac have significantly different photoperiod response (Figure 4C).

360 Since *PKCdelta* is located on the X-chromosome, both of the *PKCdelta* mutants contain
361 hemizygous males and homozygous females. The CCR was performed to determine whether there
362 will be a difference in photoperiod response between hemizygous and homozygous flies under SD
363 and LD photoperiod. Both *PKCdelta*:MIC and *PKCdelta*:Pbac mutants show a difference in
364 photoperiod response between hemizygous and homozygous flies (Figure S8). To determine if
365 there was a difference in period phenotype between hemizygous and homozygous flies in the
366 *PKCdelta*:Pbac and MIC mutants, we performed the period assay. We found no significant
367 difference between the period phenotype between hemizygous and homozygous flies (Figure 4D).
368 WT flies have an expected period of 24 hr with no difference between hemizygous and
369 homozygous flies (t-test, p > 0.05). *PKCdelta*:MIC hemizygous flies have a period of 30 hr and
370 homozygous flies have a period of 29 hr but there was no statistically significant difference
371 between hemizygous and homozygous flies (t-test, p > 0.05). There was no significant difference
372 between hemizygous and homozygous flies of *PKCdelta*:Pbac in the circadian period (t-test, p >

373 0.05). Based on these data together, we concluded that MIC mutant allele affected the ability to
374 distinguish between LD from SD, and also altered the circadian period.

375 Next, we predicted that *PKCdelta*:Pbac has knockdown of all three transcripts of
376 *PKCdelta*, while *PKCdelta*:MIC has knockdown of RC & RD based on the reported locations of
377 the insertion. The RE isoform is believed to be mainly responsible for photoperiod response
378 because the *PKCdelta*:MIC mutant shows a decrease in the photoperiod response in the CCR and
379 diapause assays. We also predicted that the transcripts RC and RD could play a role in interpreting
380 photoperiod response, though they might not be major players in interpreting photoperiods. These
381 predictions were then confirmed by performing a qPCR experiment using the *PKCdelta*:MIC and
382 *PKCdelta*:Pbac mutants under SD and LD condition (Fig.5).

383

384 *Expression of PKCdelta*

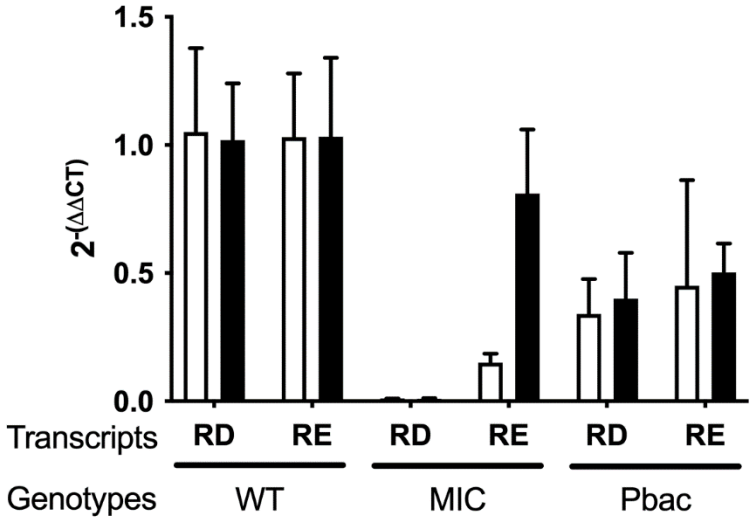

Figure 5. Expression level of *PKCdelta* allelic mutants under LD (open) and SD (filled) compared to DGRP 208 WT. In the WT flies there is no difference in expression of RD and RE transcripts under LD and SD (n=3-5, t-test, $p > 0.05$). In *PKCdelta*:MIC the expression of RD

is significantly reduced compared to WT (n=3-5, t-test, $p<0.001$). However, there is a reduction of RE transcript under LD compared to SD in *PKCdelta*:MIC (n=3-5, t-test, $p < 0.001$). In the *PKCdelta*:Pbac background, the expression of RD and RE is overall reduced compared to WT (n=3-5, t-test, $p<0.05$). There was no statistical difference in the expression levels under LD and SD photoperiods (n=3-5, t-test, $p > 0.05$).

We measured the expression levels of *PKCdelta* under different photoperiod conditions (Materials and Methods). WT flies under LD and SD photoperiods did not show statistically significant change in *PKCdelta* RD and RE transcript levels (t-test, $p > 0.05$). *PKCdelta*:MIC which was predicted to have reduced expression of RD and normal expression of RE, show overall decrease in expression of RD in both LD and SD (t-test, $p > 0.05$). However, there is an alteration in the expression levels of the RE between the photoperiod conditions in *PKCdelta*:MIC. The *PKCdelta:*MIC mutant under LD show a significant decrease in its expression level from that of SD (t-test, $p < 0.001$). *PKCdelta*:Pac mutant show an overall decrease in RD and RE expression from that of WT (t-test $p < 0.05$). Though there is no significant difference in the expression levels of RD and RE between the photoperiods in *PKCdelta*:Pac mutant, (t-test $p > 0.05$). This suggests that there is an alteration in the expression of the RE transcript in the *PKCdelta:*MIC mutant due to long day photoperiod condition. Based on this data and the diapause data, we concluded that RD transcript could be involved in distinguishing between SD and LD. Since *PKCdelta*:MIC which has reduced expression of RD transcript show no difference in the diapause response between photoperiods (Figure 4A & 5). Alternatively, the *PKCdelta*:Pbac mutant which has reduced expression of both transcripts shows a greater proportion of diapause response compared

402 to WT in both LD and SD suggesting that expression *PKCdelta* and diapause response is
403 negatively correlated in this mutant.

404 Next, we reasoned that the GWAS analysis of the DGRP CCR response itself as a trait
405 under LD and SD conditions will lead us identifying the downstream genes involved in CCR. We
406 performed the GWAS analysis on the CCR trait as a phenotype rather than the photoperiodic
407 response (CD values) as a trait discussed earlier (Files S4 - S7). There were six genes that were
408 highly associated with the CCR phenotypes both in SD and LD conditions: *Sif, Comm2, Bru-3,*
409 *Fife*, *CG32111* and *Spab*. *Sif* is involved in actin cytoskeleton organization; visual perception and
410 it localizes to the synapse. *Comm2* is essential for nerve cord development and axon guidance.
411 *Bru*-3 is known to mediate mRNA translation repression. While *Fife* is responsible for encoding
412 synaptic scaffolding protein, which promotes neurotransmitter release. *CG32111* is a long non-
413 coding RNA though much information is not known about this gene. *Spab* is a protein coding gene
414 from the neuropeptide gene group, however not much is known about this gene (Flybase.org). As
415 expected, most of the genes responsible for the CCR response play a role in the nervous system.
416 However, *Sif* and *CG32111* are known to be a target of the circadian clock transcription complex
417 CLK/CYC, suggesting that CCR photoperiod response could be regulated by the clock (Abruzzi
418 et al., 2011). *Sif* is also known to interact with *Fas2* which than interacts with *PKCdelta* (Rees et
419 al., 2011).

420

421 **Discussion**

422 In this study, we were able to establish that there is a variation in photoperiod response measured
423 by the CCR phenotype within the DGRP population. By calculating the effect size (Cohen's D
424 value) for each DGRP genotype we determined how each genotype's photoperiod response was

425 different from one another. The GWAS analysis on CD values allowed us to narrow down the 32
426 photoperiod candidate genes. We chose 4 top candidate photoperiod genes for genetic analysis.
427 The allelic mutant of *PKCdelta* showed a significantly different photoperiod response from WT.
428 To test the necessity of the gene for the photoperiodic response, we analyzed two different mutant
429 alleles: *PKCdelta*:Pbac and *PKCdelta*:MIC. By performing a qPCR assay under LD and SD it was
430 confirmed that *PKCdelta*:Pbac has decreased expression of RD and RE transcripts of the gene.
431 The *PKCdelta*:MIC mutant which show reduced expression of the RD transcript, show a
432 photoperiod effect under LD in the RE transcript levels. The CCR assay showed that
433 *PKCdelta*:Pbac mutants have a greater effect size compared to *PKCdelta*:MIC. Finally, to test the
434 hypothesis whether there is an overlap in the genetic mechanisms between the circadian clock and
435 photoperiodism, the circadian periods of our candidate genes were analyzed. *GlcAT-P* knockout
436 and *PKCdelta*;MIC mutants had a significantly longer period phenotype from the WT. Our data
437 supports the view that *PKCdelta* is involved in both circadian clock and photoperiodism.

438 Diapause and CCR are two different output pathways that are under the photoperiod
439 regulation in insects. Our data showed that the two different mutant alleles of *PKCdelta* manifested
440 the altered photoperiod response in different ways. The flies with *PKCdelta*:MIC allele could not
441 distinguish LD from SD, whereas the flies with *PKCdelta*:Pbac allele had an elevated instances of
442 diapause under both photoperiods (Figure 4A). The CCR data suggests that the *PKCdelta*:Pbac
443 mutation plays a role in increasing the sensitivity to photoperiod in the flies overall. Both the
444 mutants have positive CD values indicting their recovery time was faster than that of WT. While
445 *PKCdelta*:Pbac compared to *PKCdelta*:MIC has a greater effect size (Figure 4B).

446 Taken together, we have a working model for the photoperiodism in *D. melanogaster*. The
447 photoperiod candidate gene *PKCdelta* is hypothesized to be regulated by the clock. There are

448 certain genetic components that are under clock control which interact with *PKCdelta.* The
449 circadian transcription complex CLK/CYC is known to directly regulates the *Mef2* transcription
450 which then has been identified to target *Fas2*. *Mef2* is known for its role in myogenesis and
451 development (Sivachenko et al., 2013). However, *Mef2* is shown to be present in clock neurons
452 and fluctuation in *Mef2* are rhythmic (Sivachenko et al., 2013). *Mef2* is a major component of the
453 CLK/CYC, which is important for circadian behavior of neuronal morphology. A Chip-Chip
454 analysis determined that *Fascilin2* (*Fas2*) is a direct target of *Mef2* (Sivachenko et al., 2013). *Fas2*
455 is known to be involved in neural cell adhesion, and there is a rhythmic oscillation of *Fas2* in
456 pigment-dispersing factor (PDF) cells types, suggesting that *Fas2* is under circadian clock control
457 (Sivachenko et al., 2013). *PKCdelta* is proposed to interact with *Fas2* (Rees et al., 2011). PDF is
458 known to effect *Drosophila* circadian clock where certain mutations in PDF can shorten the period
459 of certain clock neurons while lengthening the period others neurons (Wülbeck et al., 2008). The
460 diapause assay showed that *PKCdelta*:MIC mutants lose the ability to distinguish between day-
461 lengths. *PKCdelta*:MIC mutant's loss of photoperiod sensitivity is similar to the well-studied
462 PDF^{01} mutant (Ojima et al., 2018).Our data reject the model that circadian clock and
463 photoperiodism are separate entities with no shared regulations. The current study sheds light onto
464 potential genes that could be further studied to characterize the mechanisms of photoperiodism,
465 and its relationship to the circadian clock.
466

467 **Data Availability**

468 All DGRP lines are available at the Bloomington Drosophila Stock Center, and the genotype
469 information of all lines are available at http://dgrp2.gnets.ncsu.edu. The raw CCR and CD data for
470 all DGRP lines are available under File S1. The Files S2, S4, & S6 contain the top GWAS

associations along with qq-plots, and input data used to obtain the GWAS results from CD, LD, and SD data sets. The Files S3, S5, & S7 contain all associations found in the GWAS study using the CD, LD and SD data sets. All Supplemental Materials are available at figShare portal, gsajournals.figshare.com.

Acknowledgements

The authors are grateful for Drs. Nir Yakoby, Nathan Fried, and Charot Rodeget for critical reading and insightful suggestions. We are grateful for the Lee lab members, especially Sienna Casciato and Somya Patro, for helpful discussions. The authors would also like to thank Cody Stevens for helping us navigate through some of the challenging aspects of the project. The work was funded by the NIH MARC U-STAR, T34GM127154.

Supplemental Material

Figure S1. The distribution of core 38 set DGRP parent strains.

Figure S2. Sex difference in CCR assay among the select DGRP strains.

Figure S3. The Gene enrichment results of the 32 hits using flymodEnrichr.

Figure S4. Diagram of the two *PKCdelta* mutant alleles, Pbac and MIC.

Figure S5. Overview of the *PKCdelta* gene structure and the position of the oligos for PCR products.

Figure S6. Sequence variations in *PKCdelta* RE transcript.

Figure S7. Phylogenetic analysis of *PKCdelta* RE transcript.

Figure S8. Cohen's D and Genome Effect Size of *PKCdelta* mutants.

Figure S9. The regulatory and catalytic domains of *PKCdelta*.

494 **Table S1.** The top 32 hits of the GWAS analysis sorted by the significant p values.

495 **Table S2.** Oligos used in the current study.

496 **Table S3.** Predicted changes *PKCdelta*:Pbac mutant.

497 **Table S4.** Predicted changes in *PKCdelta*:MIC mutant.

498 **File S1**. Raw CCR and Cohen's D data for all the DGRP lines. It's divided into three tabs;

499 Cohen's values, CCR in LD and CCR in SD.

500 **File S2**. TOP GWAS hits along with images of QQ plots.

501 **File S3**. SNP associations found in the GWAS study.

502 **File S4**. TOP GWAS hits using the CCR data in LD.

503 **File S5**. All GWAS hits using the CCR data in LD.

504 **File S6**. TOP GWAS hits using the CCR data in SD.

505 **File S7**. All GWAS hits using the CCR data in SD.

506

507

508 **References**

509 Abruzzi, K.C., Rodriguez, J., Menet, J.S., Desrochers, J., Zadina, A., Luo, W., Tkachev, S., and

510 Rosbash, M. (2011). Drosophila CLOCK target gene characterization: implications for

511 circadian tissue-specific gene expression. Genes & Development *25*, 2374–2386.

512 Bradshaw, W.E., and Holzapfel, C.M. (2010). What Season Is It Anyway? Circadian Tracking

513 vs. Photoperiodic Anticipation in Insects. J. Biol. Rhythms *25*, 155–165.

514 Carstensen, M.B., Hertz, H., Bering, T., Møller, M., Rohde, K., Klein, D.C., Coon, S.L., and

515 Rath, M.F. (2019). Circadian regulation and molecular role of the *Bsx* homeobox gene in

516 the adult pineal gland. J. Pineal Res.

517 Chiu, J.C., Low, K.H., Pike, D.H., Yildirim, E., and Edery, I. (2010). Assaying Locomotor
518 Activity to Study Circadian Rhythms and Sleep Parameters in Drosophila. JoVE J. Vis.
519 Exp. e2157.
520 Dubowy, C.M., and Cavanaugh, D.J. (2014). Sleep: A Neuropeptidergic Wake-Up Call for Flies.
521 Curr. Biol. *24*, R1092–R1094.
522 Harbison, S.T., Kumar, S., Huang, W., McCoy, L.J., Smith, K.R., and Mackay, T.F.C. (2019).
523 Genome-Wide Association Study of Circadian Behavior in Drosophila melanogaster.
524 Behav. Genet. *49*, 60–82.
525 Hosler, J.S., Burns, J.E., and Esch, H.E. (2000). Flight muscle resting potential and species-
526 specific differences in chill-coma. J. Insect Physiol. *46*, 621–627.
527 Huang, W., Massouras, A., Inoue, Y., Peiffer, J., Ramia, M., Tarone, A.M., Turlapati, L.,
528 Zichner, T., Zhu, D., Lyman, R.F., et al. (2014). Natural variation in genome architecture
529 among 205 Drosophila melanogaster Genetic Reference Panel lines. Genome Res. *24*,
530 1193–1208.
531 Johnson, C.H., Zhao, C., Xu, Y., and Mori, T. (2017). Timing the day: what makes bacterial
532 clocks tick? Nat Rev Microbiol *15*, 232–242.
533 Johansson, M., and Staiger, D. (2015). Time to flower: interplay between photoperiod and the
534 circadian clock. Journal of Experimental Botany *66*, 719–730.
535 Kim, B.-T., Tsuchida, K., Lincecum, J., Kitagawa, H., Bernfield, M., and Sugahara, K. (2003).
536 Identification and Characterization of Three Drosophila melanogaster
537 Glucuronyltransferases Responsible for the Synthesis of the Conserved
538 Glycosaminoglycan-Protein Linkage Region of Proteoglycans. J. Biol. Chem. *278*, 9116–
539 9124.

540 Kumar, A. (2009). An Overview of Nested Genes in Eukaryotic Genomes. Eukaryot. Cell *8*,
541 1321–1329.
542 Lanciani, C.A., Lipp, K.E., and Giesel, J.T. (1992). The effect of photoperiod on cold tolerance
543 in Drosophila melanogaster. Journal of Thermal Biology *17*, 147–148.
544 Larkin A, Marygold SJ, Antonazzo G, Attrill H, dos Santos G, Garapati PV, Goodman JL,
545 Gramates LS, Millburn G, Strelets VB, Tabone CJ, Thurmond J and the FlyBase
546 Consortium (2021) FlyBase: updates to the Drosophila melanogaster knowledge
547 base. Nucleic Acids Res. 49(D1) D899–D907
548 Lees, A.D. (1960). Some Aspects of Animal Photoperiodism. Cold Spring Harb. Symp. Quant.
549 Biol. *25*, 261–268.
550 Mackay, T.F.C., Richards, S., Stone, E.A., Barbadilla, A., Ayroles, J.F., Zhu, D., Casillas, S.,
551 Han, Y., Magwire, M.M., Cridland, J.M., et al. (2012). The Drosophila melanogaster
552 Genetic Reference Panel. Nature *482*, 173–178.
553 Martinez-Bakker, M., Bakker, K.M., King, A.A., and Rohani, P. (2014). Human birth
554 seasonality: latitudinal gradient and interplay with childhood disease dynamics. Proc. R.
555 Soc. B Biol. Sci. *281*, 20132438.
556 Maruani, J., Anderson, G., Etain, B., Lejoyeux, M., Bellivier, F., and Geoffroy, P.A. (2018). The
557 neurobiology of adaptation to seasons: Relevance and correlations in bipolar disorders.
558 Chronobiol. Int. *35*, 1335–1353.
559 Mukai, A., and Goto, S.G. (2016). The clock gene period is essential for the photoperiodic
560 response in the jewel wasp Nasonia vitripennis (Hymenoptera: Pteromalidae). Applied
561 Entomology and Zoology *51*, 185–194.

562 Nagy, D., Andreatta, G., Bastianello, S., Martín Anduaga, A., Mazzotta, G., Kyriacou, C.P., and
563 Costa, R. (2018). A Semi-natural Approach for Studying Seasonal Diapause in
564 Drosophila melanogaster Reveals Robust Photoperiodicity. J. Biol. Rhythms *33*, 117–
565 125.
566 Ojima, N., Hara, Y., Ito, H., and Yamamoto, D. (2018). Genetic dissection of stress-induced
567 reproductive arrest in Drosophila melanogaster females. PLOS Genetics *14*, e1007434.
568 Ortavant, R., Mauleon, P., and Thibault, C. (1964). Photoperiodic Control of Gonadal and
569 Hypophyseal Activity in Domestic Mammals. Ann. N. Y. Acad. Sci. *117*, 157–193.
570 Pegoraro, M., Gesto, J.S., Kyriacou, C.P., and Tauber, E. (2014). Role for circadian clock genes
571 in seasonal timing: testing the Bünning hypothesis. PLoS Genet. *10*, e1004603.
572 Saunders, D.S. (1990). The Circadian Basis of Ovarian Diapause Regulation in Drosophila
573 melanogaster: Is the period Gene Causally Involved in Photoperiodic Time
574 Measurement? J. Biol. Rhythms *5*, 315–331.
575 Saunders, D.S. (2012). Insect photoperiodism: seeing the light. Physiol. Entomol. *37*, 207–218.
576 Saunders, D.S., Henrich, V.C., and Gilbert, L.I. (1989). Induction of diapause in Drosophila
577 melanogaster: photoperiodic regulation and the impact of arrhythmic clock mutations on
578 time measurement. Proc. Natl. Acad. Sci. *86*, 3748–3752.
579 Sawa, M., Kay, S.A., and Imaizumi, T. (2008). Photoperiodic flowering occurs under internal
580 and external coincidence. Plant Signal. Behav. *3*, 269–271.
581 Shieh, B.-H., Parker, L., and Popescu, D. (2002). Protein Kinase C (PKC) Isoforms in
582 Drosophila. J. Biochem. (Tokyo) *132*, 523–527.
583 Song, Y.H., Ito, S., and Imaizumi, T. (2010). Similarities in the circadian clock and
584 photoperiodism in plants. Curr Opin Plant Biol *13*, 594–603.

585 Song, Y.H., Kubota, A., Kwon, M.S., Covington, M.F., Lee, N., Taagen, E.R., Laboy Cintrón, D.,
586 Hwang, D.Y., Akiyama, R., Hodge, S.K., et al. (2018). Molecular basis of flowering under
587 natural long-day conditions in Arabidopsis. Nat. Plants *4*, 824–835.
588 Sivachenko, A., Li, Y., Abruzzi, K.C., and Rosbash, M. (2013). The transcription factor Mef2, links the
589 Drosophila core clock to Fas2, neuronal morphology and circadian behavior. Neuron *79*.
590 Suh, K.S., Tatunchak, T.T., Crutchley, J.M., Edwards, L.E., Marin, K.G., and Yuspa, S.H.
591 (2003). Genomic structure and promoter analysis of PKC-δ. Genomics *82*, 57–67.
592 Tauber, E., and Kyriacou, B.P. (2001). Insect Photoperiodism and Circadian Clocks: Models and
593 Mechanisms. J. Biol. Rhythms *16*, 381–390.
594 Vaziri, P., Ryan, D., Johnston, C.A., and Cripps, R.M. (2020). A Novel Mechanism for
595 Activation of Myosin Regulatory Light Chain by Protein Kinase C-Delta in *Drosophila*.
596 Genetics *216*, 177–190.
597 Venken, K.J.T., Schulze, K.L., Haelterman, N.A., Pan, H., He, Y., Evans-Holm, M., Carlson,
598 J.W., Levis, R.W., Spradling, A.C., Hoskins, R.A., et al. (2011). MiMIC: a highly
599 versatile transposon insertion resource for engineering Drosophila melanogaster genes.
600 Nat. Methods *8*, 737–743.
601 Wülbeck, C., Grieshaber, E., and Helfrich-Förster, C. (2008). Pigment-Dispersing Factor (PDF)
602 Has Different Effects on Drosophila's Circadian Clocks in the Accessory Medulla and in
603 the Dorsal Brain. J. Biol. Rhythms *23*, 409–424.
604
605

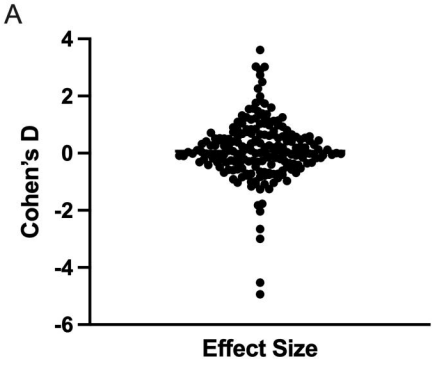
A
Cohen's D
4
2
0
-2
-4
-6
Effect Size

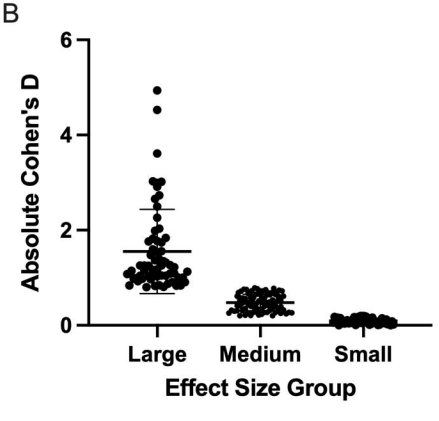
B
Absolute Cohen's D
6
4
2
0
Large
Medium
Small
Effect Size Group

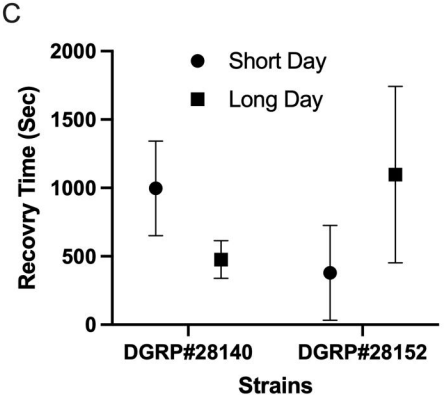
C
Short Day
Long Day
Recovry Time (Sec)
2000
1500
1000
500
0
DGRP#28140
DGRP#28152
Strains

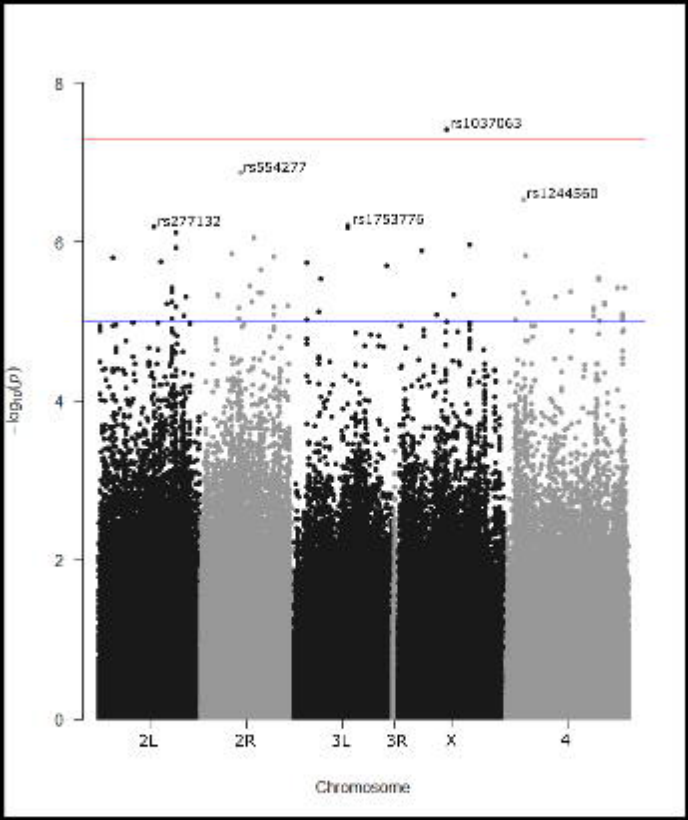
8
6
4
2
0
−log10(p)
rs1037063
rs554277
rs1244560
rs277132
rs1753776
2L
2R
3L
3R
X
4
Chromosome

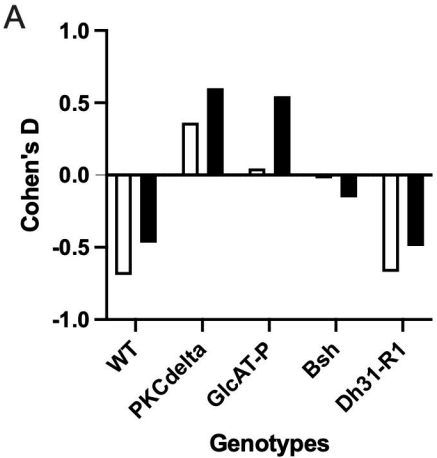
A
1.0
0.5
0.0
-0.5
-1.0
Cohen's D
WT
PKCdelta
GlcAT-P
Bsh
Dh31-R1
Genotypes

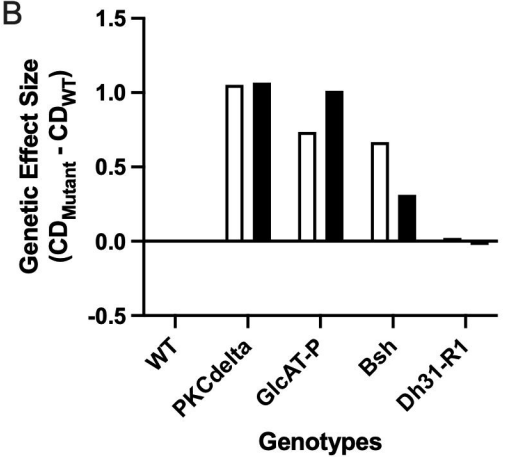
B
1.5
1.0
0.5
0.0
-0.5
Genetic Effect Size
(CD$_{Mutant}$ - CD$_{WT}$)
WT
PKCdelta
GlcAT-P
Bsh
Dh31-R1
Genotypes

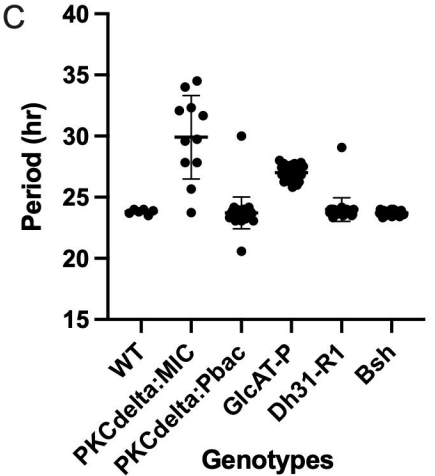
C
40
35
30
25
20
15
Period (hr)
WT
PKCdelta:MIC
PKCdelta:Pbac
GlcAT-P
Dh31-R1
Bsh
Genotypes

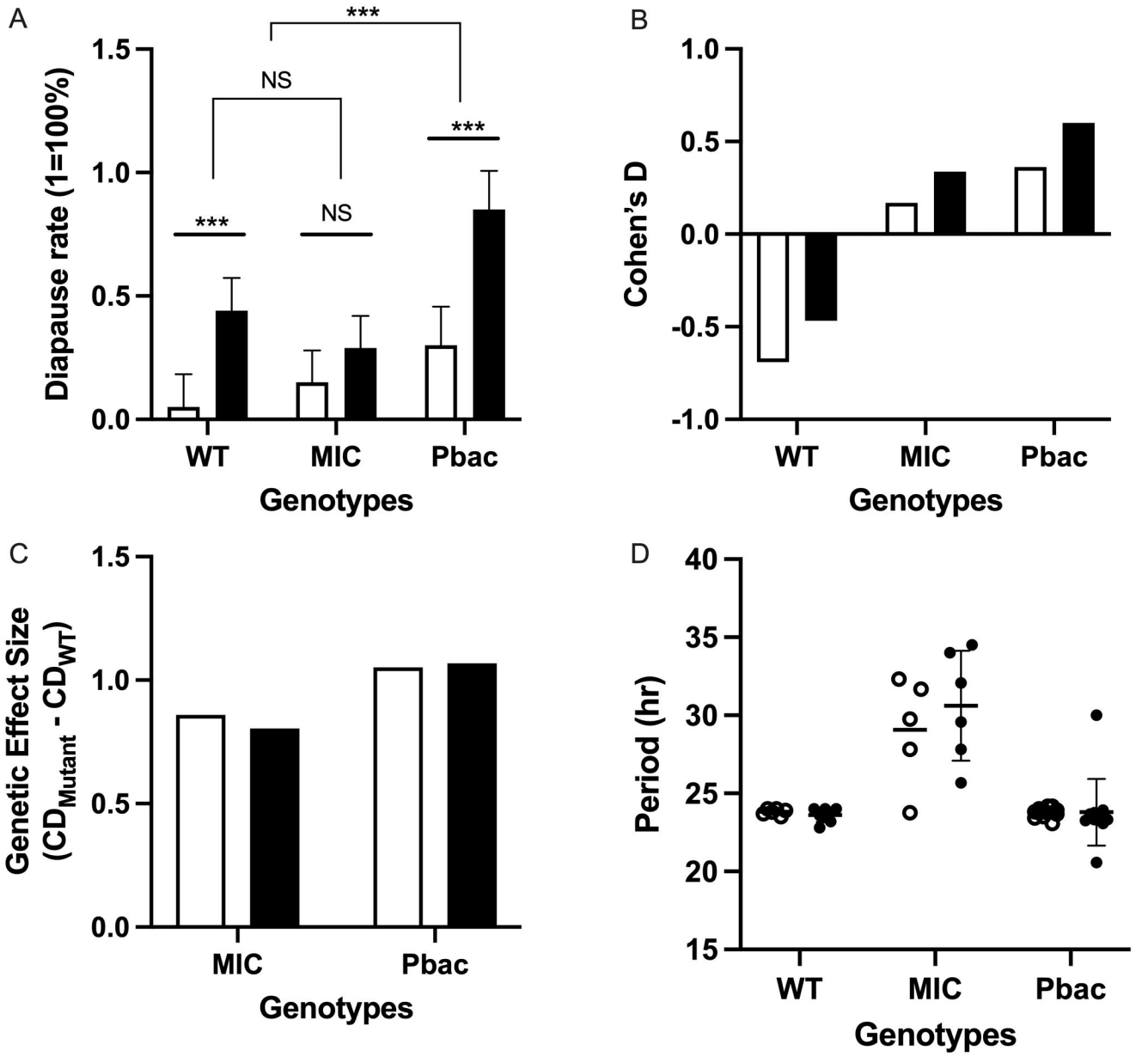
A
***
NS
***
***
NS
1.5
1.0
0.5
0.0
Diapause rate (1=100%)
WT
MIC
Pbac
Genotypes
B
1.0
0.5
0.0
-0.5
-1.0
Cohen's D
WT
MIC
Pbac
Genotypes
C
1.5
1.0
0.5
0.0
Genetic Effect Size
(CD_Mutant - CD_WT)
MIC
Pbac
Genotypes
D
40
35
30
25
20
15
Period (hr)
WT
MIC
Pbac
Genotypes

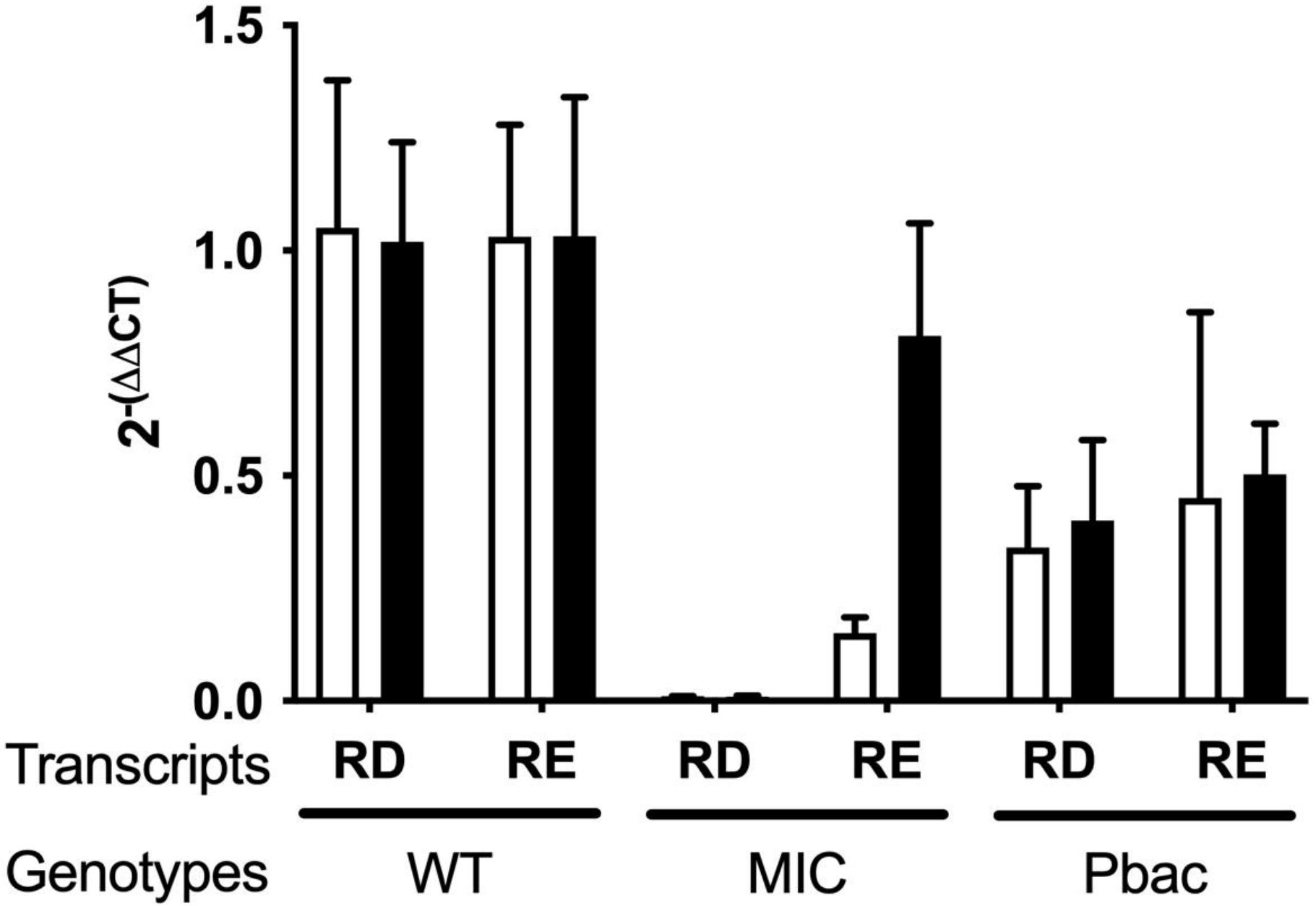
1.5
1.0
0.5
0.0
2-(ΔΔCT)
Transcripts
RD
RE
RD
RE
RD
RE
Genotypes
WT
MIC
Pbac